

# Hard scattering at RHIC: Experimental review \*

David d'Enterria <sup>†</sup>

Nevis Laboratories, Columbia University  
Irvington, NY 10533, and New York, NY 10027, USA.

## Abstract

The most significant results on hard scattering processes in Au+Au, p+p, and d+Au collisions at  $\sqrt{s_{NN}} = 200$  GeV obtained after 3 years of operation at the BNL Relativistic Heavy-Ion Collider (RHIC) are summarized. Hadron production at high transverse momentum ( $p_T$ ) in central Au+Au collisions shows very different properties (production yields, flavor composition, azimuthal correlations, ...) in comparison to p+p, d+Au, and peripheral Au+Au collisions, and this fact constitutes arguably the most interesting outcome of the experimental program so far. Four main topics are covered in this report: (i) the depletion of high  $p_T$  inclusive hadron spectra, (ii) the “anomalous” baryon-meson composition at intermediate  $p_T$ 's, (iii) the disappearance of away-side azimuthal (jet) correlations, and (iv) the large value of collective azimuthal (elliptic flow) correlations. Additionally, the observed high  $p_T$  “Cronin enhancement” in d+Au collisions will be discussed. A succinct comparison of experimental data to theoretical models is also provided.

## 1. Introduction

Heavy-ion collisions at RHIC collider energies aim at the study of QCD matter at extreme energy densities. The driving force of this research program is the study of the transition from hadronic matter to a deconfined, chirally symmetric plasma of quarks and gluons (QGP) predicted to occur above a critical energy density  $\epsilon \approx 0.7 \pm 0.3$  GeV/fm<sup>3</sup> by lattice QCD calculations [1]. Additionally, the combination of high-energies and large nuclear systems in the initial-state provides propitious grounds for the study of the regime of non-linear many-body parton (mostly gluon) dynamics at small- $x$  where saturation effects are expected to play a dominant role [2]. The most interesting phenomena observed so far in Au+Au reactions at  $\sqrt{s_{NN}} = 130$  and 200 GeV are in the high transverse momentum ( $p_T \gtrsim 2$  GeV/ $c$ ) sector where the production of hadrons in central collisions shows substantial differences compared to more elementary reactions either in the “vacuum” (p+p,  $e^+e^-$ ) or in a cold nuclear matter environment (d+Au).

Several arguments make of hard scattering processes an excellent experimental probe in heavy-ion collisions:

- They occur in the first instants of the reaction process ( $\tau \sim 1/p_T \lesssim 0.1$  fm/ $c$ ) in parton-parton scatterings with large  $Q^2$  and, thus, constitute direct probes of the partonic phase(s) of the reaction.
- A direct comparison to the baseline “vacuum” (p+p) production yields is straightforward after scaling by the nuclear geometry (in the simplest approach, this is done scaling by the nuclear overlap function  $T_{AB}$  or, equivalently, by the number of nucleon-nucleon ( $NN$ ) binary inelastic collisions,  $N_{coll} = T_{AB} \cdot \sigma_{NN}$ , given by a Glauber model).
- The production yields of high  $p_T$  particles are theoretically calculable via perturbative (or classical-field) QCD methods.

Thus, high  $p_T$  particles constitute experimentally and theoretically well calibrated observables that are sensitive to the properties of the dense QCD medium existing in central heavy-ion collisions.

---

\* Contribution to the CERN Yellow Report on Hard Probes in Heavy Ion Collisions at the LHC

<sup>†</sup> denterria@nevis.columbia.edu

The main observations so far at RHIC are the following:

- The high  $p_T$  yields of inclusive charged hadrons and  $\pi^0$  in central Au+Au at  $\sqrt{s_{NN}} = 130$  [3, 4, 5] and 200 GeV [6, 7, 8, 9, 10], are suppressed by as much as a factor 4 – 5 compared to p+p and peripheral Au+Au yields scaled by  $T_{AB}$  (or  $N_{coll}$ ).
- At intermediate  $p_T$ 's ( $p_T \approx 2. - 4.$  GeV/c) in central Au+Au, at variance with mesons ( $\pi^0$  [6] and kaons [13]) no suppression is seen for baryons ( $p, \bar{p}$  [11, 12] and  $\Lambda, \bar{\Lambda}$  [13]), yielding an “anomalous” baryon over meson ratio  $p/\pi \sim 1$  much larger than the “perturbative”  $p/\pi \sim 0.1 - 0.3$  ratio observed in p+p collisions [14, 15] and in  $e^+e^-$  jet fragmentation [16].
- The near-side azimuthal correlations of high  $p_T$  (leading) hadrons emitted in central and peripheral Au+Au reactions [17, 18] are, on the one hand, clearly reminiscent of jet-like parton fragmentation as found in p+p collisions. On the other, away-side azimuthal correlations (from back-to-back jets) in central Au+Au collisions are found to be significantly suppressed [17].
- At low  $p_T$  the strength of the azimuthal anisotropy parameter  $v_2$  is found to be large and consistent with hydrodynamical expectations for elliptic flow. Above  $p_T \sim 2$  GeV/c where the contribution from collective behaviour is negligible,  $v_2$  has still a sizeable value with a flat (or slightly decreasing) behaviour as a function of  $p_T$  [13, 19, 20].
- High  $p_T$  production in “cold nuclear matter” as probed in d+Au reactions [21, 22, 23, 10] not only is not suppressed but it is *enhanced* compared to p+p collisions, in a way very much reminiscent of the “Cronin enhancement” observed in p+A collisions at lower center-of-mass energies [24].

All these results point to strong medium effects at work in central Au+Au collisions, and have triggered extensive theoretical discussions based on perturbative or “classical”-field QCD. Most of the studies on the high  $p_T$  suppression are based on the prediction [25] that a deconfined and dense medium would induce multiple gluon radiation off the scattered partons, effectively leading to a depletion of the high- $p_T$  hadronic fragmentation products (“jet quenching”), though alternative interpretations have been also put forward based on initial-state gluon saturation effects (“Color Glass Condensate”, CGC) [2, 26], or final-state hadronic reinteractions [27]. The different behaviour of baryons and mesons at moderately high  $p_T$ 's has been interpreted, among others, in terms of “quark recombination” (or coalescence) effects in a thermalized partonic (QGP-like) medium [28], whereas the disappearance of the back-to-back azimuthal correlations can be explained in both QGP energy loss and CGC monojet scenarios. Finally, the large value of  $v_2$  above 2 GeV/c has been addressed by jet energy loss [29], gluon saturation [30], and quark recombination [31] models.

This summary report presents the  $p_T$ ,  $\sqrt{s_{NN}}$ , centrality, particle-species, and rapidity dependence of the inclusive high  $p_T$  particle production, plus the characteristics of the produced jets and collective elliptic flow signals extracted from the azimuthal correlations at large  $p_T$ , as measured by the four experiments at RHIC (BRAHMS, PHENIX, PHOBOS and STAR) in Au+Au, p+p, and d+Au collisions. The whole set of experimental data puts strong constraints on the different proposed physical explanations for the underlying QCD medium produced in heavy-ion collisions at RHIC and at LHC energies.

## 2. High $p_T$ hadron production in p+p collisions at $\sqrt{s} = 200$ GeV

### 2.1 p+p inclusive cross-sections:

Proton-proton collisions are the baseline “vacuum” reference to which one compares the Au+Au results in order to extract information about the QCD medium properties. At  $\sqrt{s} = 200$  GeV, there currently exist three published measurements of high  $p_T$  hadron cross-sections in  $p + p(\bar{p})$  collisions: UA1  $p + \bar{p} \rightarrow h^\pm$  ( $|\eta| < 2.5$ ,  $p_T < 7$  GeV/c) [32], PHENIX  $p + p \rightarrow \pi^0$  ( $|\eta| < 0.35$ ,  $p_T < 14$  GeV/c) [33], and STAR  $p + p \rightarrow h^\pm$  ( $|\eta| < 0.5$ ,  $p_T < 10$  GeV/c) [7]. At  $\sqrt{s} = 130$  GeV, an interpolation between the ISR inclusive charged hadron cross-section and UA1 and FERMILAB data, has been also used as a reference

for Au+Au at this value of  $\sqrt{s}$ . Globally the spectra can be reasonably well parametrized by a power-law form  $A \cdot (1 + p_T/p_0)^{-n}$  with the parameters<sup>1</sup> reported in Table 2.1.

system	$\sqrt{s}$ (GeV)	$p_T^{min}$ (GeV/c)	$A$ (mb GeV <sup>-2</sup> c <sup>3</sup> )	$p_0$ (GeV/c)	$n$
$p + p \rightarrow h^\pm$ (inel., interpolation [3])	130	0.4	330	1.72	12.40
$p + \bar{p} \rightarrow h^\pm$ (NSD, UA1) [32]	200	0.25	286	1.80	12.14
$p + p \rightarrow h^\pm$ (NSD, STAR) [7]	200	0.4	286	1.43	10.35
$p + p \rightarrow \pi^0$ (inel., PHENIX) [33]	200	1.0	386	1.22	9.99

Table 1: Parameters of the fit  $E d^3\sigma/dp^3 = A \cdot (1 + p_T/p_0)^{-n}$  to the inclusive  $p_T$  distributions of all existing  $p + p(\bar{p})$  hadron (inelastic or non-singly diffractive) cross-sections measurements at  $\sqrt{s} = 200$  GeV.

In general, all experimental results are consistent within each other, although it is claimed [7] that STAR p+p inclusive charged yield is smaller by a factor of  $0.79 \pm 0.18$  compared to UA1  $p + \bar{p}$  results (approximately independent of  $p_T$ ), the difference due in large part to differing non-singly-diffractive<sup>2</sup> (NSD) cross section measured ( $35 \pm 1$  mb [32] in the first and  $30.0 \pm 3.5$  mb [7] in the later). Standard next-to-leading-order (NLO) perturbative QCD calculations describe well the available high  $p_T$  p+p data at  $\sqrt{s} = 200$  GeV (see Fig. 1 for  $\pi^0$ ).

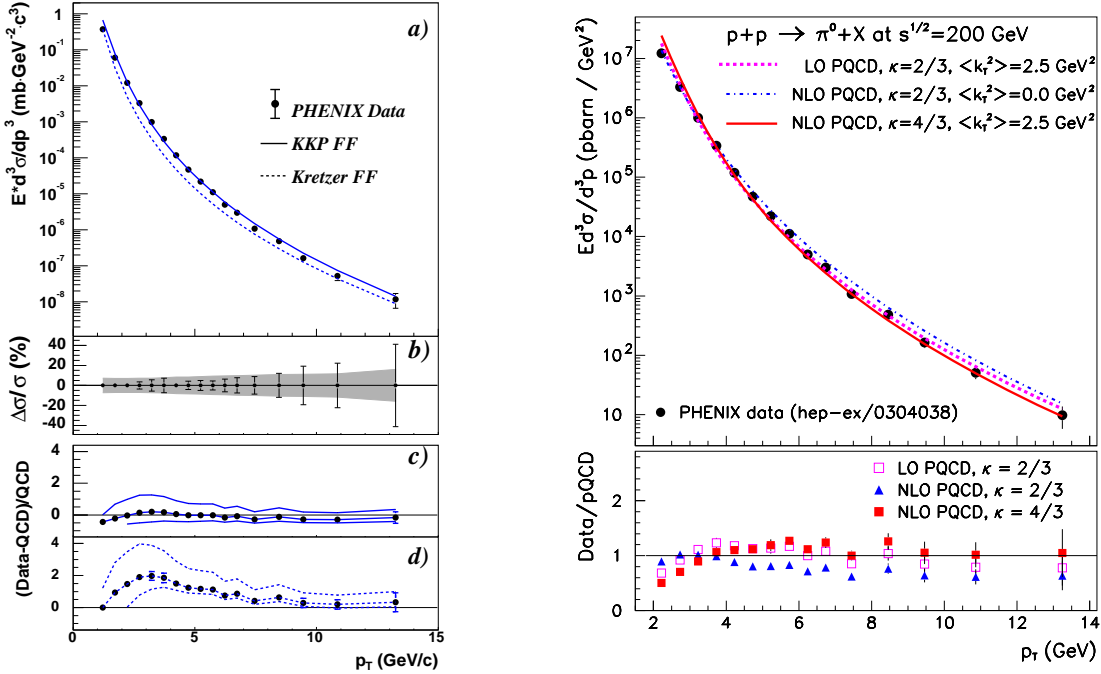


Fig. 1: High  $p_T$   $\pi^0$  cross-section in p+p collisions at  $\sqrt{s} = 200$  GeV (PHENIX) compared to the results of two different NLO PQCD calculations: [33] (left), [34] (right).

## 2.2 p+p azimuthal correlations:

PHENIX [35] has studied the azimuthal correlations at high  $p_T$  in p+p collisions at  $\sqrt{s} = 200$  GeV extracting several parameters characterizing the produced jets:

- Mean jet fragmentation transverse momentum:  $\langle |j_{\perp y}| \rangle = 373 \pm 16$  MeV/c, in agreement with previous measurements at ISR [36] and showing no significant trend with increasing  $\sqrt{s}$ .

<sup>1</sup>The fit parameters  $p_0$  and  $n$  are actually strongly correlated via the mean  $p_T$  of the collision:  $\langle p_T \rangle = 2p_0/(n - 3)$ .

<sup>2</sup>PHENIX high  $p_T$   $\pi^0$  cross-section is inclusive and contains, in principle, all inelastic (including diffractive) channels.

- Average parton transverse momentum (fitted to a constant above 1.5 GeV/c):  $\langle |k_{\perp y}| \rangle = 725 \pm 34$  MeV/c. The momentum of the pair  $p_{\perp}$  is related to the individual parton  $\langle |k_{\perp y}| \rangle$  via  $\sqrt{\langle |p_{\perp}^2| \rangle_{pair}} = \sqrt{2\pi} \langle |k_{\perp y}| \rangle$ . The extracted  $\sqrt{\langle |p_{\perp}^2| \rangle_{pair}} = 1.82 \pm 0.85$  GeV/c is in agreement with the existing systematics of dimuon, diphoton and dijet data in hadronic collisions [37].

### 3. High $p_T$ hadron production yields in Au+Au collisions

There is a significant amount of high  $p_T$  Au+Au experimental spectra ( $p_T > 2$  GeV/c) measured by the 4 experiments at RHIC: inclusive charged hadrons at 130 [3, 4, 5] and 200 GeV [7, 8, 9, 10], neutral pions at 130 [3] and 200 GeV [6], protons and antiprotons at 130 [11] and 200 GeV [12],  $K_s^0$  at 200 GeV [13], and  $\Lambda, \bar{\Lambda}$  at 200 GeV [13]. Moreover, all these spectra are measured for different centrality bins and permit to address the impact parameter dependence of high  $p_T$  production.

Details on hadron production mechanisms in  $AA$  are usually studied via their scaling behavior with respect to p+p collisions. On the one hand, soft processes ( $p_T < 1$  GeV/c) are expected to scale with the number of participating nucleons  $N_{part}$  [38] (and they actually approximately do [39, 40]). On the other, in the framework of collinear factorization, hard processes are incoherent and thus expected to scale with  $N_{coll}$ .

The first interesting result at RHIC in the high  $p_T$  sector is the *breakdown* of this  $N_{coll}$  scaling for central Au+Au collisions. Fig. 2 shows the comparison of the p+p  $\pi^0$  spectrum to peripheral (left) and central (right) Au+Au spectra, and to pQCD calculations. Whereas peripheral data is consistent with a simple superposition of individual  $NN$  collisions, central data shows a suppression factor of 4 – 5 with respect to this expectation.

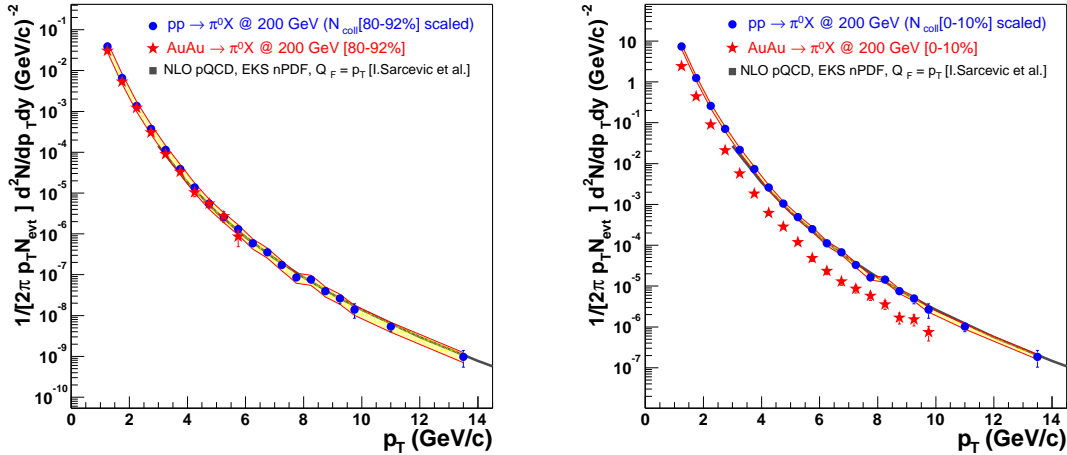


Fig. 2: Invariant  $\pi^0$  yields measured by PHENIX in peripheral (*left*) and in central (*right*) Au+Au collisions (stars), compared to the  $N_{coll}$  scaled p+p  $\pi^0$  yields (circles) and to a NLO pQCD calculation [41] (gray line). The yellow band around the scaled p+p points includes in quadrature the absolute normalization errors in the p+p and Au+Au spectra as well as the uncertainties in  $T_{AB}$ . Updated version of Fig. 1 of [42] with final published data [6, 33].

It is customary to quantify the medium effects at high  $p_T$  using the *nuclear modification factor* given by the ratio of the  $AA$  to the p+p invariant yields scaled by the nuclear geometry ( $T_{AB}$ ):

$$R_{AA}(p_T) = \frac{d^2 N_{AA}^{\pi^0} / dy dp_T}{\langle T_{AB} \rangle \times d^2 \sigma_{pp}^{\pi^0} / dy dp_T}. \quad (1)$$

$R_{AA}(p_T)$  measures the deviation of  $AA$  from an incoherent superposition of  $NN$  collisions in terms of suppression ( $R_{AA} < 1$ ) or enhancement ( $R_{AA} > 1$ ).

### 3.1 High $p_T$ suppression: magnitude and $p_T$ dependence

Figure 3 shows  $R_{AA}(p_T)$  for  $h^\pm$  (STAR [7], left) and  $\pi^0$  (PHENIX [6], right) measured in peripheral (upper points) and central (lower points) Au+Au reactions at  $\sqrt{s_{NN}} = 200$  GeV. As seen in Fig. 2, peripheral collisions are consistent<sup>3</sup> with p+p collisions plus  $N_{coll}$  scaling as well as with standard pQCD calculations [43, 44], while central Au+Au are clearly suppressed by a factor  $\sim 4 - 5$ .

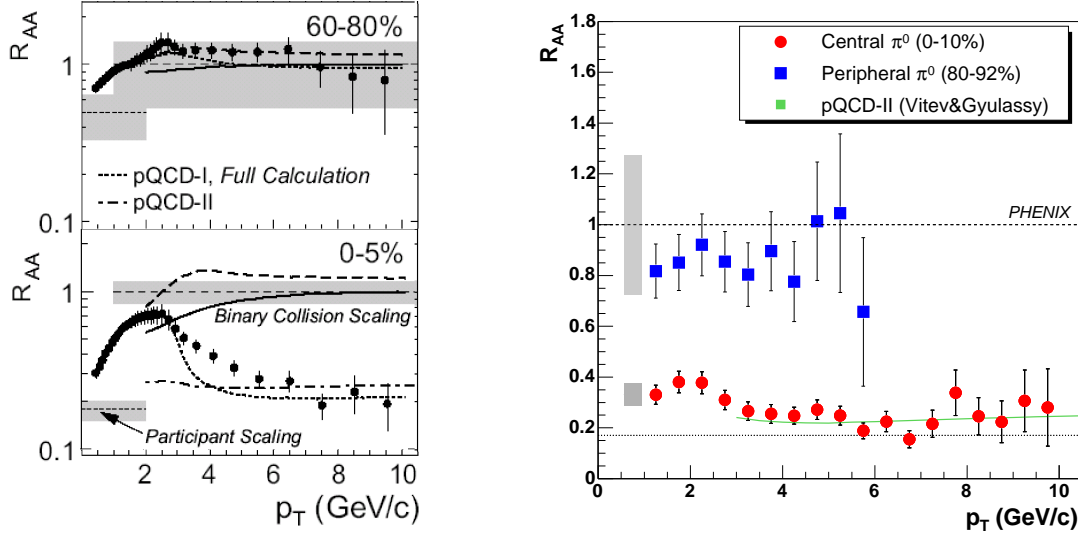


Fig. 3: Nuclear modification factor,  $R_{AA}(p_T)$ , in peripheral and central Au+Au reactions for charged hadrons (*left*) and  $\pi^0$  (*right*) measured at  $\sqrt{s_{NN}} = 200$  GeV by STAR and PHENIX respectively. A comparison to theoretical curves: pQCD-I [43], pQCD-II [44], is also shown.

The high  $p_T$  suppression in central collisions for both  $\pi^0$  and  $h^\pm$  is smallest at  $p_T = 2$  GeV/c and increases to an approximately constant suppression factor of  $1/R_{AA} \approx 4 - 5$  over  $p_T = 5 - 10$  GeV/c. Above 5 GeV/c the data are consistent within in errors with “participant scaling” given by the dotted line at  $R_{AA} \approx 0.17$  in both plots (actually both STAR and PHENIX data are systematically slightly above this scaling). The magnitude and  $p_T$  dependence of  $R_{AA}$  in the range  $p_T = 1 - 10$  GeV/c (corresponding to parton fractional momenta  $x_{1,2} = p_T/\sqrt{s}(e^{\pm y_1} + e^{\pm y_2}) \approx 2p_T/\sqrt{s} \sim 0.02 - 0.1$  at midrapidity), is alone inconsistent with “conventional” nuclear effects like leading-twist shadowing of the nuclear parton distribution functions (PDFs) [48, 49]. Different pQCD-based jet quenching calculations [43, 44, 45, 34, 46] based on medium-induced radiative energy loss, can reproduce the *magnitude* of the  $\pi^0$  suppression assuming the formation of a hot and dense partonic system characterized by different, but related, properties: i) large initial gluon densities  $dN^g/dy \sim 1000$  [43], ii) large “transport coefficients”  $\hat{q}_0 \sim 3.5$  GeV/fm<sup>2</sup> [45], iii) high opacities  $L/\lambda \sim 3 - 4$  [34], or iv) effective parton energy losses of the order of  $dE/dx \sim 14$  GeV/fm [44].

The  $p_T$  dependence of the quenching predicted by all models that include the QCD version of the Landau-Pomeranchuk-Migdal (LPM) interference effect (BDMPS [50] and GLV [51] approaches) is a slowly (logarithmic) increasing function of  $p_T$ , a trend not compatible with the data over the entire measured  $p_T$  range. Other approaches, such as constant energy loss per parton scattering, are also not supported as discussed in [41]. Analyses which combine LPM jet quenching together with shadowing and initial-state  $p_T$  broadening (“pQCD-II” [43] in Fig. 3) globally reproduce the observed flat  $p_T$  dependence of  $R_{AA}$ , as do recent approaches that take into account detailed balance between parton emission and absorption (“pQCD-I” [44] in Fig. 3, left).

At variance with parton energy loss descriptions, a gluon saturation calculation [26] is able to predict the magnitude of the observed suppression, although it fails to reproduce exactly the flat  $p_T$

<sup>3</sup>Although peripheral STAR charged hadron data seems to be slightly above  $R_{AA} = 1$  and PHENIX  $\pi^0$  data seems to be below, within errors both measurements are consistent with “collision scaling”.

dependence of the quenching [7]. Similarly, *semi-quantitative* estimates of final-state interactions in a dense *hadronic* medium [27] yield the same amount of quenching as models based on partonic energy loss, however it is not yet clear whether the  $p_T$  evolution of the hadronic quenching factor is consistent with the data or not [7, 53].

The amount of suppression for  $\pi^0$  [6] and  $h^\pm$  [7, 8] is the same above  $p_T \approx 4 - 5$  GeV/c for all centrality classes [8]. However, below  $p_T \sim 5$  GeV/c,  $\pi^0$ 's are more suppressed than inclusive charged hadrons in central collisions (as can be seen by comparing the right and left plots of Fig. 3). This is due to the enhanced baryon production contributing to the total charged hadron yield in the intermediate  $p_T$  region ( $p_T \approx 1 - 4$  GeV/c) in Au+Au collisions [12, 13] (see section 3.4 below).

### 3.2 High $p_T$ suppression: $\sqrt{s_{NN}}$ dependence

Figure 4 shows  $R_{AA}(p_T)$  for several  $\pi^0$  measurements in high-energy  $AA$  collisions at different center-of-mass energies [52]. The PHENIX  $R_{AA}(p_T)$  values for central Au+Au collisions at 200 GeV (circles) and 130 GeV (triangles) are noticeably below unity in contrast to the enhanced production ( $R_{AA} > 1$ ) observed at CERN-ISR (min. bias  $\alpha + \alpha$  [15], stars) and CERN-SPS energies (central Pb+Pb [47], squares) and interpreted in terms of initial-state  $p_T$  broadening (“Cronin effect” [24]).

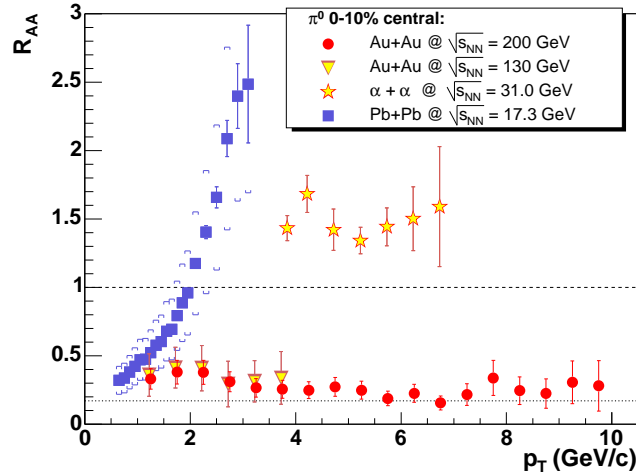


Fig. 4: Nuclear modification factor,  $R_{AA}(p_T)$ , for  $\pi^0$  measured in central ion-ion reactions at CERN-SPS [47] (squares), CERN-ISR [15] (stars), and BNL-RHIC (triangles [3], circles [6]) energies.

Figure 5 shows  $R_{200/130}(p_T)$ , the ratio of Au+Au charged hadron yields at  $\sqrt{s_{NN}} = 130$  and 200 GeV in 4 centrality classes, compared to pQCD and gluon saturation model predictions [7]. The increase in high  $p_T$  yields between the two center-of-mass energies is a factor  $\sim 2$  at the highest  $p_T$ 's, whereas at low  $p_T$ , the increase is much moderate, of the order of 15%. The large increment of the hard cross sections is naturally consistent with pQCD expectations due to the increased jet contributions at high transverse momenta. In the saturation model [26] the increase at high  $p_T$  is accounted for by the enhanced gluon densities at  $\sqrt{s_{NN}} = 200$  GeV compared to 130 GeV in the “anomalous dimension”  $x_T$  region of the Au parton distribution function.

PHENIX [8] has addressed the  $\sqrt{s}$  dependence of high  $p_T$  production by testing the validity of “ $x_T$  scaling” in Au+Au, i.e. verifying the parton model prediction that hard scattering cross sections can be factorized in 2 terms depending on  $\sqrt{s}$  and  $x_T = 2p_T/\sqrt{s}$  respectively:

$$E \frac{d^3\sigma}{dp^3} = \frac{1}{p_T^{n(\sqrt{s})}} F(x_T) \implies E \frac{d^3\sigma}{dp^3} = \frac{1}{\sqrt{s}^{n(x_T, \sqrt{s})}} G(x_T). \quad (2)$$

In (2),  $F(x_T)$  embodies all the  $x_T$  dependence coming from the parton distribution (PDF) and frag-

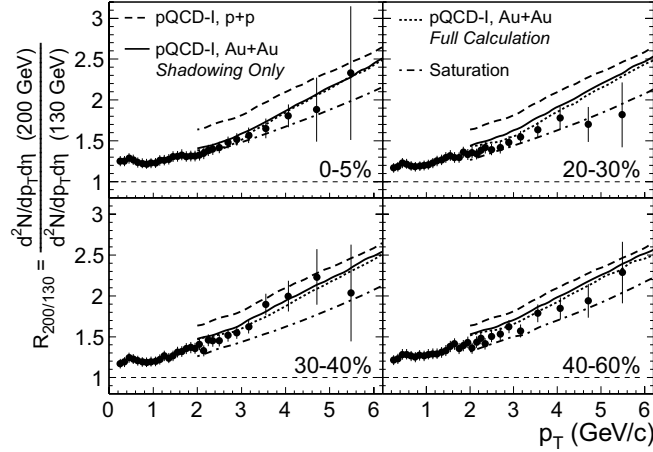


Fig. 5:  $R_{200/130}(p_T)$  vs.  $p_T$  for  $(h^+ + h^-)/2$  for four different centrality bins measured by STAR compared to pQCD and gluon saturation model predictions [7].

mentation (FF) functions<sup>4</sup>, while the exponent  $n$ , related to the underlying parton-parton scattering, is measured to be  $n \approx 4 - 8$  in a wide range of  $p + p, \bar{p}$  collisions [8]. Fig. 6 compares the  $x_T$ -scaled hadron yields in  $\sqrt{s_{NN}} = 130$  GeV and 200 GeV Au+Au central and peripheral collisions. According to Eq. (2), the ratio of inclusive cross-sections at fixed  $x_T$  should equal  $(200/130)^n$ . On the one hand,  $x_T$  scaling holds<sup>5</sup> in Au+Au with the same scaling power  $n = 6.3 \pm 0.6$  for neutral pions (in central and peripheral collisions) and charged hadrons (in peripheral collisions) as measured in p+p [8]. This is consistent with equal (pQCD-like) production dynamics in p+p and Au+Au, and disfavours final-state effects described with medium-modified FF's that violate  $x_T$  scaling (e.g. constant parton energy losses independent of the parton  $p_T$ ). Equivalently, models that predict strong initial-state effects (e.g. gluon saturation) respect  $x_T$  scaling as long as their predicted modified nuclear PDFs are depleted, independently of  $\sqrt{s}$ , by the same amount at a given  $x_T$  (and centrality). On the other hand, Fig. 6 (right) shows that charged hadrons in central collisions (triangles) break  $x_T$  scaling which is indicative of a non perturbative modification of particle composition spectra from that of p+p at intermediate  $p_T$ 's (see section 3.4 below).

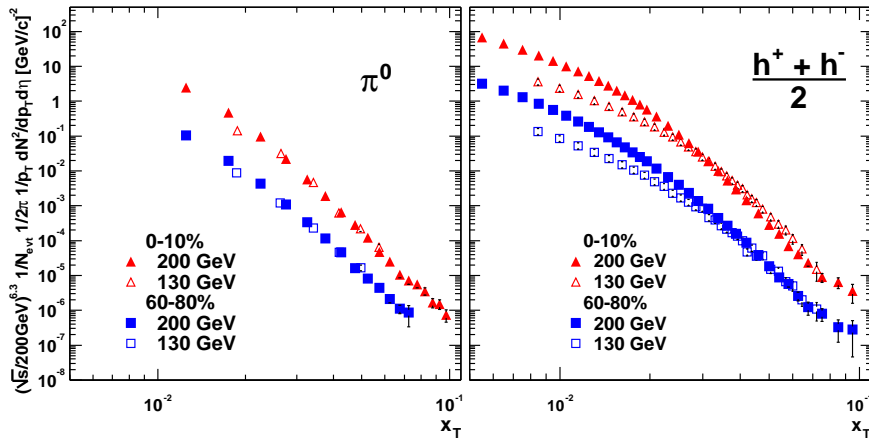


Fig. 6:  $x_T$  scaled spectra for  $\pi^0$  (left) and  $(h^+ + h^-)/2$  (right) measured in central and peripheral collisions at  $\sqrt{s_{NN}} = 130$  and 200 GeV by PHENIX [8]. Central (Peripheral)  $x_T$  spectra are represented by triangles (squares), and solid (open) symbols represent  $x_T$  spectra from  $\sqrt{s_{NN}} = 200$  GeV ( $\sqrt{s_{NN}} = 130$  GeV scaled by a factor of  $[130/200]^{6.3}$ ).

<sup>4</sup>PDFs and FFs, to first order, scale as the ratio of  $p_T$  at different  $\sqrt{s}$ .

<sup>5</sup>In the kinematical region,  $x_T > 0.03$ , where pQCD is expected to hold.

### 3.3 High $p_T$ suppression: centrality dependence

In each centrality bin, the value of the high  $p_T$  suppression can be quantified by the ratio of Au+Au over  $N_{coll}$ -scaled p+p yields integrated above a given (large enough)  $p_T$ . The centrality dependence of the high  $p_T$  suppression for  $\pi^0$  and charged hadrons, given by  $R_{AA}(p_T > 4.5 \text{ GeV}/c)$ , is shown in Fig. 7 (left) as a function of  $\langle N_{part} \rangle$  for PHENIX data. The transition from the  $N_{coll}$  scaling behaviour ( $R_{AA} \sim 1$ ) apparent in the most peripheral region,  $\langle N_{part} \rangle \lesssim 40$ , to the strong suppression seen in central reactions ( $R_{AA} \sim 0.2$ ) is smooth. Whether there is an abrupt or gradual departure from  $N_{coll}$  scaling in the peripheral range cannot be ascertained within the present experimental uncertainties [52]. The data, however, is inconsistent with  $N_{coll}$  scaling (at a  $2\sigma$  level) for the 40–60% centrality corresponding to  $\langle N_{part} \rangle \approx 40 - 80$  [5, 52], whose estimated ‘‘Bjorken’’ energy density ( $\epsilon_{Bj} \approx 1 \text{ GeV}/\text{fm}^3$ ) [52] is in the ball-park of the expected ‘‘critical’’ QCD energy density. A similar centrality dependence of the high  $p_T$  suppression is seen in STAR  $h^\pm$  data (Fig. 7, right)

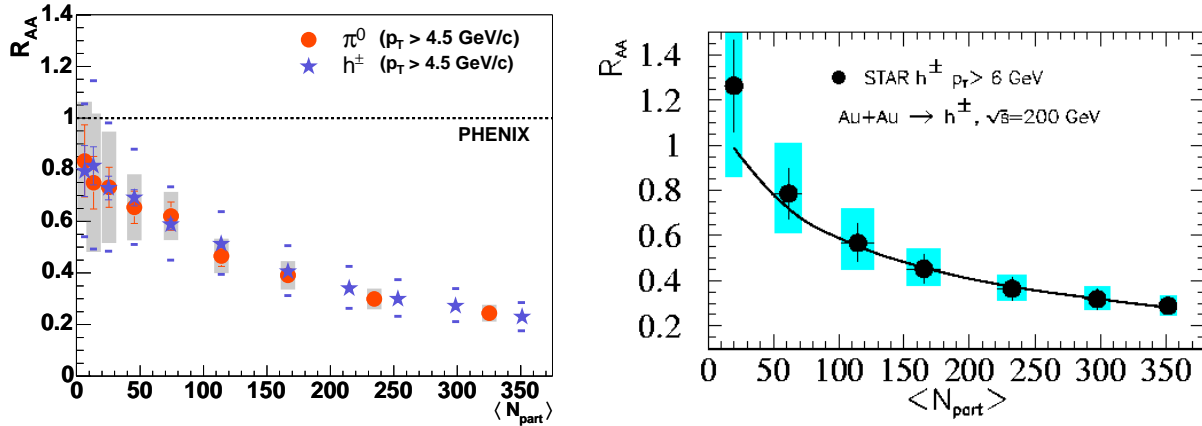


Fig. 7: Evolution of the high  $p_T$   $\pi^0$  and  $h^\pm$  suppression,  $R_{AA}(p_T > 4.5 \text{ GeV}/c)$ , as a function of centrality given by  $\langle N_{part} \rangle$  (PHENIX, left). Same evolution shown as  $R_{AA}(p_T > 6.0 \text{ GeV}/c)$  for STAR  $h^\pm$  data [53] (right).

$N_{part}$  (instead of  $N_{coll}$ ) scaling at high  $p_T$  is expected in scenarios dominated either by gluon saturation [26] or by surface emission of the quenched jets [54]. ‘‘Approximate’’  $N_{part}$  scaling has been claimed by PHOBOS [9]: the ratio of central to a fit to mid-central yields in the range  $p_T \approx 2 - 4 \text{ GeV}/c$  stays flat as a function of centrality (Fig. 8, left). However, at higher  $p_T$  values, where the suppression is seen to saturate at its maximum value, the centrality dependence of the ratio of  $N_{part}$ -scaled Au+Au over p+p yields for  $\pi^0$  and  $h^\pm$  measured by PHENIX (Fig. 8, right) does not show a true participant scaling ( $R_{AA}^{part} > 1$  for all centralities). Nonetheless, the fact that the production per participant pair above  $4.5 \text{ GeV}/c$  is, within errors, approximately constant over a wide range of intermediate centralities, is in qualitative agreement with a gluon saturation model prediction [26].

### 3.4 High $p_T$ suppression: particle species dependence

One of the most intriguing results of the RHIC program so far is the different suppression pattern of baryons and mesons at moderately high  $p_T$ 's. Figure 9 (left) compares the  $N_{coll}$  scaled central to peripheral yield ratios<sup>6</sup> for  $(p + \bar{p})/2$  and  $\pi^0$ :  $R_{cp} = (\text{yield}^{(0-10\%)} / N_{coll}^{0-10\%}) / (\text{yield}^{(60-92\%)} / N_{coll}^{60-92\%})$ . From 1.5 to 4.5  $\text{GeV}/c$  the (anti)protons are not suppressed ( $R_{cp} \sim 1$ ) at variance with the pions which are reduced by a factor of 2 – 3 in this  $p_T$  range. If both  $\pi^0$  and  $p, \bar{p}$  originate from the fragmentation of hard-scattered partons that lose energy in the medium, the nuclear modification factor  $R_{cp}$  should be independent of particle species contrary to the experimental result. The same discussion applies for strange mesons and baryons as can be seen from the right plot of Fig. 9. Whereas the kaon yields in

<sup>6</sup>Since the 60–92% peripheral Au+Au (inclusive and identified) spectra scale with  $N_{coll}$  when compared to the p+p yields [6, 7, 12],  $R_{cp}$  carries basically the same information as  $R_{AA}$ .

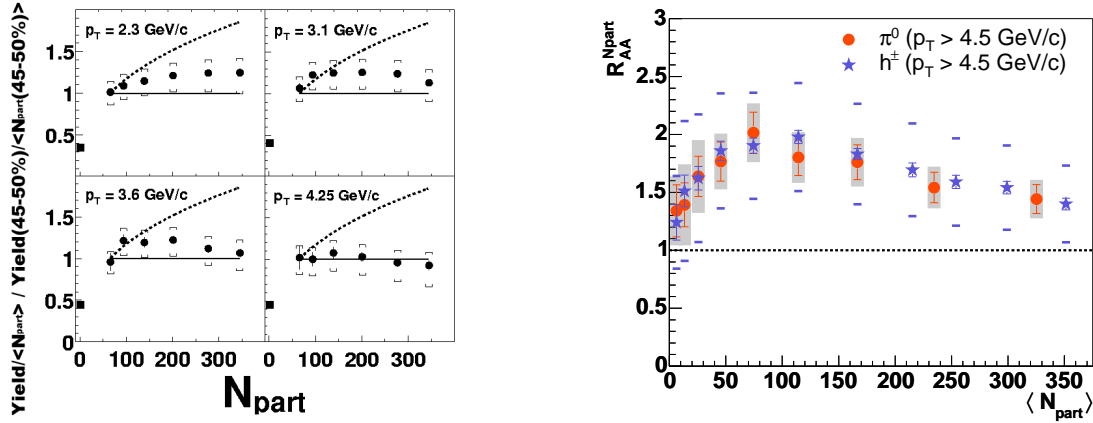


Fig. 8: *Left*: Ratio of central to semi-central  $h^\pm$  yields normalized by  $N_{part}$  in 4 different  $p_T$  bins, as a function of  $N_{part}$  measured by PHOBOS [9]. The dashed (solid) line shows the expectation for  $N_{coll}$  ( $N_{part}$ ) scaling. *Right*: Ratio of Au+Au over p+p  $\pi^0$  and  $h^\pm$  yields above 4.5 GeV/c normalized by  $N_{part}$  ( $R_{AA}^{N_{part}}$ ) as a function of centrality given by  $\langle N_{part} \rangle$  as measured by PHENIX [6, 8]. The dashed line indicates the expectation for  $N_{part}$  scaling.

central collisions are suppressed with respect to “ $N_{coll}$  scaling” for all measured  $p_T$ , the yield of  $\Lambda + \bar{\Lambda}$  is close to expectations from collision scaling in the  $p_T$  range 1.8 – 3.5 GeV/c. Interestingly, above  $p_T \sim 5.0$  GeV/c, the  $K_S^0, K^\pm, \Lambda + \bar{\Lambda}$ , and charged hadron yields are suppressed from binary scaling by a similar factor.

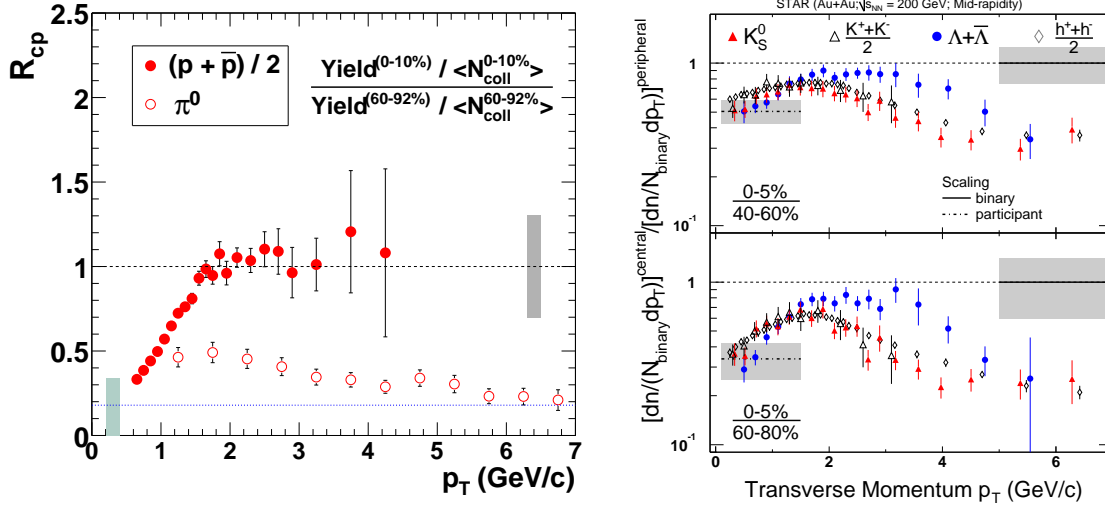


Fig. 9: Ratio of central over peripheral  $N_{coll}$  scaled yields,  $R_{cp}(p_T)$ , as a function of  $p_T$  for different species measured in Au+Au collisions:  $(p + \bar{p})/2$  (dots) and  $\pi^0$  (circles) by PHENIX [12] (*left*), and  $\Lambda, \bar{\Lambda}$  (circles) and  $K_S^0, K^\pm$  (triangles) by STAR [13] (*right*).

Figure 10 (left) shows the ratios of  $(p + \bar{p})/2$  over  $\pi^0$  as a function of  $p_T$  measured by PHENIX in central (0–10%, circles), mid-central (20–30%, squares), and peripheral (60–92%, triangles) Au+Au collisions [12], together with the corresponding ratios measured in p+p collisions at CERN-ISR energies [14, 15] (crosses) and in gluon and quark jet fragmentation from  $e^+e^-$  collisions [16] (dashed and solid lines resp.). Within errors, peripheral Au+Au results are compatible with the p+p and  $e^+e^-$  ratios, but central Au+Au collisions have a  $p/\pi$  ratio  $\sim 4 - 5$  times larger. Such a result is at odds with standard perturbative production mechanisms, since in this case the particle ratios  $\bar{p}/\pi$  and  $p/\pi$  should

be described by a universal fragmentation function independent of the colliding system, which favors the production of the lightest particle. Beyond  $p_T \approx 4.5$  GeV/c, the identification of charged particles is not yet possible with the current PHENIX configuration, however the measured  $h/\pi^0 \sim 1.6$  ratio above  $p_T \sim 5$  GeV/c in central and peripheral Au+Au is consistent with that measured in p+p collisions (Fig. 10, right). This result together with STAR  $R_{cp}$  result on strange hadrons (Fig. 9, right) supports the fact that for large  $p_T$  values the properties of the baryon production mechanisms approach the (suppressed) meson scaling, thus limiting the observed baryon enhancement in central Au+Au collisions to the intermediate transverse momenta  $p_T \lesssim 5$  GeV/c.

Several theoretical explanations (see refs. in [11, 12]) have been proposed to justify the different behaviour of mesons and baryons at intermediate  $p_T$ 's based on: (i) quark recombination (or coalescence), (ii) medium-induced difference in the formation time of baryons and mesons, (iii) different ‘‘Cronin enhancement’’ for protons and pions, or (iv) ‘‘baryon junctions’’. In the recombination picture [28] the partons from a thermalized system coalesce and with the addition of quark momenta, the soft production of baryons extends to much larger values of  $p_T$  than that for mesons. In this scenario, the effect is limited to  $p_T < 5$  GeV, beyond which fragmentation becomes the dominant production mechanism for all species.

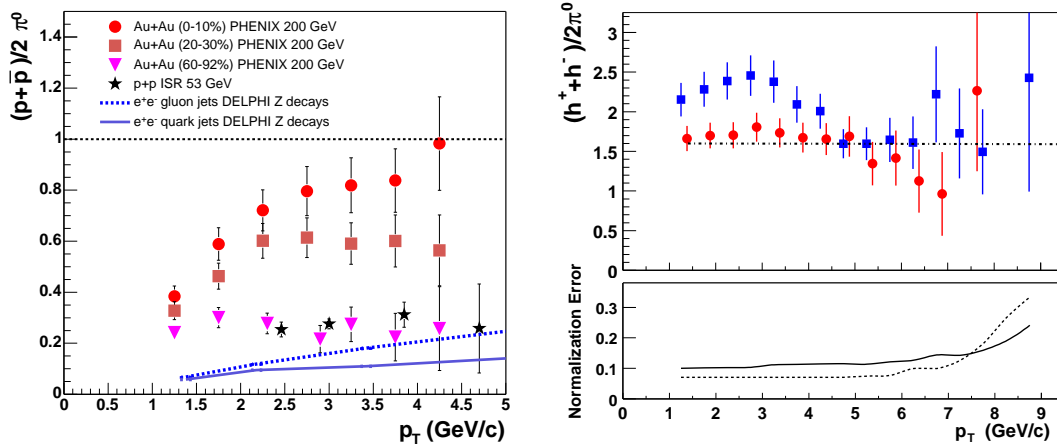


Fig. 10: *Left*: Ratios of  $(p + \bar{p})/2$  over  $\pi^0$  versus  $p_T$  in central (dots), mid-central (squares), and peripheral (triangles) Au+Au, and in p+p (crosses), and  $e^+e^-$  (dashed and solid lines) collisions [12]. *Right*: Ratio of charged hadron to  $\pi^0$  in central (0–10% - squares) and peripheral (60–92% - circles) Au+Au collisions compared to the  $h/\pi \sim 1.6$  ratio (dashed-dotted line) measured in p+p collisions [12].

### 3.5 High $p_T$ suppression: pseudorapidity dependence

BRAHMS is, so far, the only experiment at RHIC that has measured high  $p_T$  inclusive charged hadron spectra off mid-rapidity. Fig. 11 (left) shows the nuclear modification factors  $R_{AA}(p_T)$  for central and semi-peripheral Au+Au measurements at mid-pseudorapidity ( $\eta = 0$ ) and at  $\eta = 2.2$  [10]. The high  $p_T$  suppression is not limited to central rapidities but it is clearly apparent at forward  $\eta$ 's too. Fig. 11 (right) shows the ratio of suppressions at the two pseudorapidity values,  $R_\eta = R_{cp}(\eta = 2.2)/R_{cp}(\eta = 0)$ . The high  $p_T$  deficit at  $\eta = 2.2$  is similar to, or even larger than, at  $\eta = 0$  indicating that the volume causing the suppression extends also in the longitudinal direction.

## 4. High $p_T$ azimuthal correlations in Au+Au collisions

There are two main sources of azimuthal correlations at high  $p_T$  in heavy-ion collisions:

- The *fragmentation* of hard-scattered *partons* results in jets of high  $p_T$  hadrons correlated in both rapidity and azimuthal angle. Such correlations are short range ( $\Delta\eta \lesssim 0.7$ ,  $\Delta\phi \lesssim 0.75$ ), involve

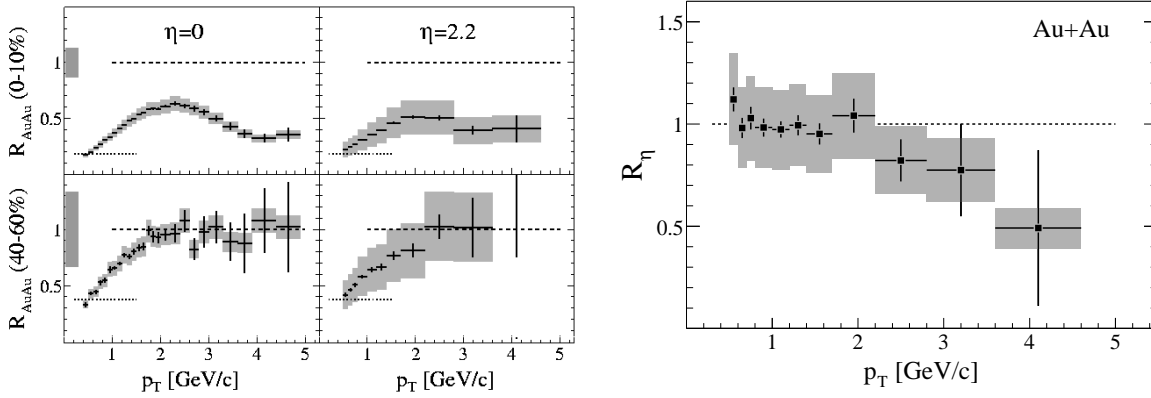


Fig. 11: *Left*:  $R_{AA}(p_T)$  measured by BRAHMS at  $\eta = 0$  and  $\eta = 2.2$  for 0–10% most central and for semi-peripheral (40-60%) Au+Au collisions. *Right*: Ratio  $R_\eta$  of  $R_{cp}$  distributions at  $\eta = 2.2$  and  $\eta = 0$ . Figs. from [10].

comparatively large transverse momentum particles ( $p_T > 2$  GeV/c), and are unrelated (in principle) to the orientation of the AA reaction plane.

- *Collective (elliptic) flow*: The combination of (i) the geometrical asymmetry in non-central AA reactions (“almond”-like region of the overlapping nuclei), and (ii) multiple reinteractions between the produced particles in the overlap region; results in pressure gradients in the collision ellipsoid which transform the original coordinate-space asymmetry into a momentum-space anisotropy. The amount of elliptic flow (a true collective effect absent in p+p collisions) is measured by the second harmonic coefficient,  $v_2 \equiv \langle \cos(2\phi) \rangle$ , of the Fourier expansion of the particles azimuthal distribution with respect to the reaction plane.

Additionally, there are other second-order sources of angular correlations like resonance decays, final state (particularly Coulomb) interactions, momentum conservation, or other experimental effects like photon conversions, which have to be subtracted out in order to extract the interesting “jet-like” or “flow-like” signals.

#### 4.1 High $p_T$ azimuthal correlations: Jet signals

Although, standard jet reconstruction algorithms fail below  $p_T \approx 40$  GeV/c when applied to the soft-background dominated environment of heavy-ion collisions, angular correlations of pairs of high  $p_T$  particles [17, 18] have been very successfully used to study on a statistical basis the properties of the produced jets. For each event with “trigger” particle(s) with  $p_T = 4 - 6$  GeV/c and “associated” particle(s) with  $p_T = 2 - 4$  GeV/c and  $|\eta| < 0.7$ , STAR [17] determines the two-particle azimuthal distribution

$$D(\Delta\phi) \propto \frac{1}{N_{trigger}} \frac{dN}{d(\Delta\phi)}. \quad (3)$$

Fig. 12 shows  $D(\Delta\phi)$  for peripheral (left) and central (right) Au+Au collisions (dots) compared to  $D(\Delta\phi)$  from p+p collisions (histogram), and to a superposed  $\cos(2\Delta\phi)$  flow-like term (blue curve). On the one hand, the correlation strength at small relative angles ( $\Delta\phi \sim 0$ ) in peripheral and central Au+Au as well as at back-to-back angles ( $\Delta\phi \sim \pi$ ) in peripheral Au+Au are very similar to the scaled correlations in p+p collisions. The near-side peaks in all three collision systems are characteristic of jet fragmentation [17] (a result also observed by PHENIX using *neutral* trigger particles [18]). On the other hand, the away-side peak ( $\Delta\phi \sim \pi$ ) in central collisions is strongly suppressed.

In order to study the evolution as a function of centrality of the the near-side,  $D^{AuAu}(\Delta\phi < 0.75)$ , and away-side,  $D^{AuAu}(\Delta\phi > 2.24)$ , angular correlations in Au+Au compared to p+p,  $D^{pp}$ , STAR has

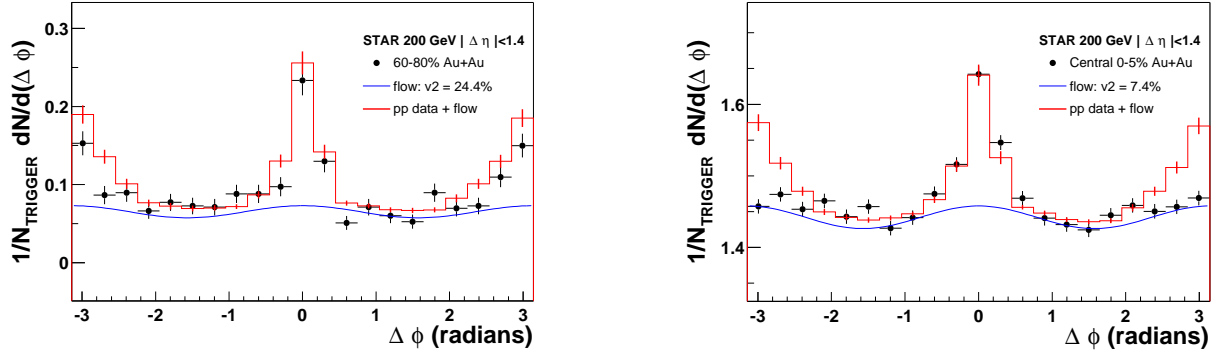


Fig. 12: Azimuthal correlations for peripheral (*left*) and central (*right*) Au+Au collisions compared to the pedestal and flow-scaled correlations in p+p collisions. Fig. from [55].

constructed the quantity

$$I_{AA}(\Delta\phi_1, \Delta\phi_2) = \frac{\int_{\Delta\phi_1}^{\Delta\phi_2} d(\Delta\phi) [D^{\text{AuAu}} - B(1 + 2v_2^2 \cos(2\Delta\phi))]}{\int_{\Delta\phi_1}^{\Delta\phi_2} d(\Delta\phi) D^{\text{pp}}}, \quad (4)$$

where  $B$  accounts for overall background and  $v_2$  the azimuthal correlations due to elliptic flow. Fig. 13 shows  $I_{AA}$  for the near-side (squares) and away-side (circles) correlations as a function of the number of participating nucleons ( $N_{part}$ ). On the one hand, the near-side correlation function is relatively suppressed compared to the expectation from Eq. (4) in the most peripheral region (a result not completely understood so far) and increases slowly with  $N_{part}$ . On the other hand, the back-to-back correlation strength above the background from elliptic flow, decreases with increasing  $N_{part}$  and is consistent with zero for the most central collisions. The disappearance of back-to-back jet-like correlations is consistent with large energy loss effects in a system that is opaque to the propagation of high-momentum partons or their fragmentation products.

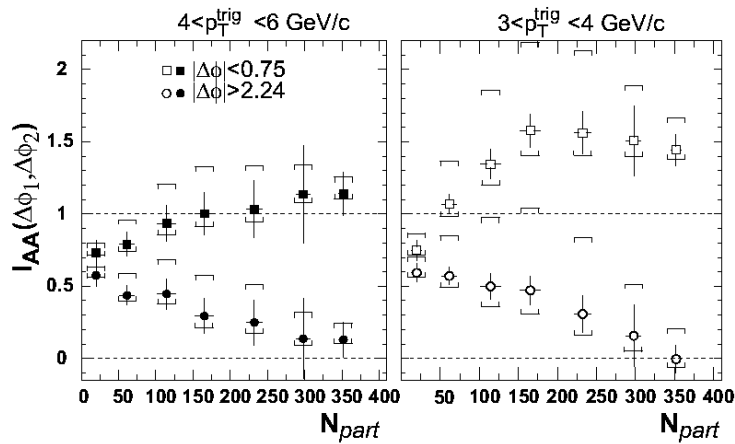


Fig. 13: Ratio of Au+Au over p+p integrated azimuthal correlations, Eq. (4), for small-angle (squares,  $|\Delta\phi| < 0.75$  radians) and back-to-back (circles,  $|\Delta\phi| > 2.24$  radians) azimuthal regions versus number of participating nucleons for trigger particle intervals  $4 < p_T^{\text{trig}} < 6$  GeV/c (solid) and  $3 < p_T^{\text{trig}} < 4$  GeV/c (hollow) [17].

## 4.2 High $p_T$ azimuthal correlations: Collective elliptic flow

At low  $p_T$  the strength of the elliptic flow signal is found to be large and consistent with hydrodynamics expectations. Above  $p_T \sim 2$  GeV/ $c$  where the contribution from collective behaviour is negligible,  $v_2$  is found to be still a sizeable signal which saturates and/or slightly decreases as a function of  $p_T$  [19, 20, 13]. The large value  $v_2(p_T > 2 \text{ GeV}/c) \sim 0.15$  implies unrealistically large parton densities and/or cross-sections according to standard parton transport calculations [31]. Various interpretations have been proposed to account for such a large  $v_2$  parameter within different physical scenarios. In jet quenching models [29] the resulting momentum anisotropy results from the almond-like density profile of the opaque medium (see, however, [56]). Calculations based on gluon saturation [30] yield a (“non-flow”) azimuthal asymmetry component from the fragmentation of the released gluons from the initial-state saturated wave functions of the colliding nuclei. Finally, quark recombination effects [31] can naturally enhance the elliptic flow of the produced hadrons compared to that of partons. The measured  $v_2(p_T)$  for mesons and baryons shows a distinct pattern (Fig. 14):  $v_2^m > v_2^b$  at low  $p_T$ ,  $v_2^m \approx v_2^b$  at  $p_T \approx 2$  GeV/ $c$ , and  $v_2^m < v_2^b$  at higher  $p_T$ 's; which further constrains the proposed theoretical explanations.

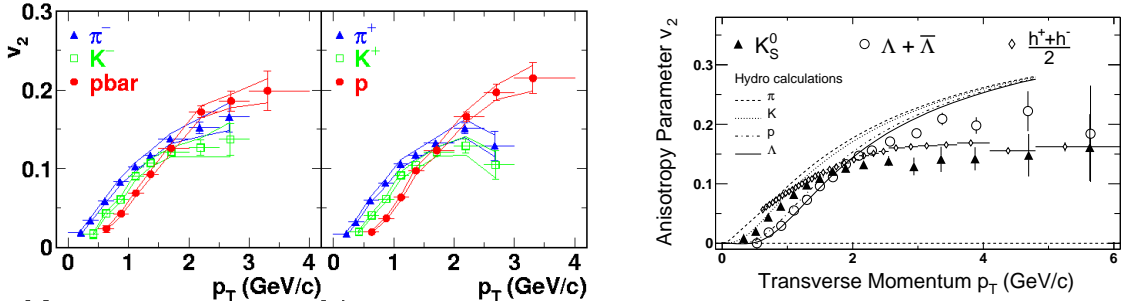


Fig. 14:  $v_2$  as a function of transverse momentum for identified particles at RHIC:  $\pi^\pm$ ,  $K^\pm$  and  $p$ ,  $\bar{p}$  from PHENIX (left), and  $K_s^0$  and  $\Lambda$ ,  $\bar{\Lambda}$  from STAR (right).

Quark coalescence models [31] naturally lead to weaker baryon flow than meson flow at low  $p_T$ , while the opposite holds above 2 GeV/ $c$ . This simple mass ordering expectation is confirmed by the identified particle data from PHENIX and STAR (Fig. 15). The fact that the  $v_2$  parameters scaled by the number of constituent quarks ( $n = 2$  for mesons,  $n = 3$  baryons) versus  $p_T/n$ , globally fall in a single curve, supports the scenario where hadrons at moderate  $p_T$ 's form by coalescence of co-moving quarks.

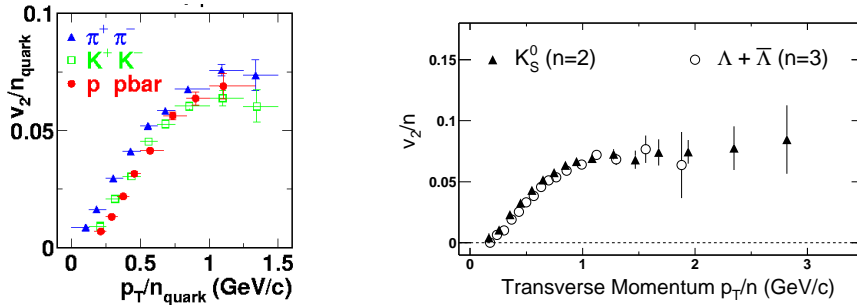


Fig. 15: The  $v_2$  parameter scaled by the number of constituent quarks ( $n$ ) versus  $p_T/n$  for  $\pi^\pm$ ,  $K^\pm$  and  $p$ ,  $\bar{p}$  (PHENIX [20], left) and  $K_s^0$  and  $\Lambda$ ,  $\bar{\Lambda}$  (STAR [13], right).

## 5. High $p_T$ hadron production in d+Au collisions

Proton- (or deuteron-) nucleus collisions constitute a reference “control” experiment needed to determine the influence of *cold* nuclear matter effects in high  $p_T$  hadro-production. Since final-state medium effects are marginal in p,d+Au collisions, they are basic tools to ascertain whether models based on initial- or final- state QCD effects can explain the distinct hard scattering behaviour observed in Au+Au collisions at RHIC. During the third year of RHIC operation, the 4 experiments collected data from d+Au collisions at  $\sqrt{s_{NN}} = 200$  GeV. The resulting high  $p_T$  results at mid-rapidity from PHENIX [21], STAR [22], PHOBOS [23], and BRAHMS [10] consistently indicate the following:

- High  $p_T$  inclusive  $h^\pm$  [21, 22, 23, 10] and  $\pi^0$  [21] spectra from d+Au minimum bias (MB) collisions are not suppressed but are *enhanced* compared to p+p collisions ( $R_{dAu}$  plots in Fig. 16), in a way very much reminiscent of the “Cronin effect” observed in fixed-target p+A collisions at lower  $\sqrt{s}$  [24]. As a matter of fact, p+Au collisions (from neutron-tagged d+Au events [21]) show a similar behaviour as minimum bias d+Au collisions.
- Above  $p_T \sim 2.5$  GeV/c the nuclear modification factor of inclusive charged hadrons in MB d+Au collisions saturates at <sup>7</sup>  $R_{dAu} \sim 1.4$ . Above 6 GeV/c, STAR  $h^\pm$  and PHENIX  $\pi^0$  results seem to indicate that  $R_{dAu}$  decreases as a function of  $p_T$ , becoming consistent with 1 at around 8 GeV/c.
- The “Cronin enhancement” for unidentified hadrons at high  $p_T$  ( $R_{dAu}^{h^\pm} \approx 1.35$ ) is larger than for neutral pions ( $R_{dAu}^{\pi^0} \approx 1.1$ ) [21].
- The degree of “enhancement” in d+Au compared to p+p *increases* with collision centrality [23, 22], an opposite trend to Au+Au results.
- The azimuthal correlations in MB and central d+Au collisions are very similar to that of p+p and do not show the significant suppression of the away-side peak observed in central Au+Au reactions [22].

All these results lead to the conclusion that no “cold” nuclear matter (or initial-state) effects, - like a strong saturation of the nuclear parton distribution functions in the relevant  $(x, Q^2)$  kinematical region probed by the current experimental setups-, can explain the high  $p_T$  behaviour in central Au+Au. The data suggest, instead, that final-state interactions are responsible of the high  $p_T$  suppression and the disappearance of back-to-back dijet correlations observed at mid-rapidity in central Au+Au reactions.

## 6. Summary

A vast body of high transverse momentum data has been collected and analyzed during 2000–2003 by the 4 experiments at RHIC in Au+Au, p+p, d+Au collisions at  $\sqrt{s_{NN}} = (130)200$  GeV. This has permitted a detailed comparative study of the properties of high  $p_T$  particle production in high-energy heavy-ion collisions as a function of  $p_T$ ,  $\sqrt{s_{NN}}$ , collision centrality, pseudo-rapidity, and particle species. All these studies reveal that hadron production at high transverse momentum in central Au+Au reactions shows significant deviations compared to p+p, d+Au, and Au+Au peripheral collisions at RHIC energies, as well as to nucleus-nucleus data at lower center-of-mass energies. The main observations are: (i) the inclusive and identified spectra are suppressed by a factor 4 – 5 above  $p_T \approx 5$  GeV/c compared to the expectations of  $N_{coll}$  scaling, (ii) the baryon yields are enhanced compared to the meson yields in the range of intermediate momenta  $p_T \approx 2 – 5$  GeV/c, (iii) the back-to-back dijet azimuthal correlations are significantly suppressed, (iv) there is a strong constant elliptic flow signal at high  $p_T$ . The whole set of results puts strong experimental constraints on the properties of the underlying QCD medium produced in Au+Au reactions at collider energies. Comparison of the energy spectra and angular correlations data to the theoretical calculations globally supports pQCD-based models of final-state parton energy loss in a dense medium, although non-perturbative effects (like e.g. quark coalescence) are needed in order to explain the baryon-meson differences in yield and  $v_2$  in the intermediate  $p_T$  window ( $p_T \approx 2 – 5$  GeV/c).

<sup>7</sup>  $R_{dAu}^{PHENIX}(p_T = 2 – 7 \text{ GeV/c}) \sim 1.35$ ,  $R_{dAu}^{STAR}(p_T = 2 – 6 \text{ GeV/c}) \sim 1.45$ ,  $R_{dAu}^{BRAHMS}(p_T = 2 – 5 \text{ GeV/c}) \sim 1.3$ .

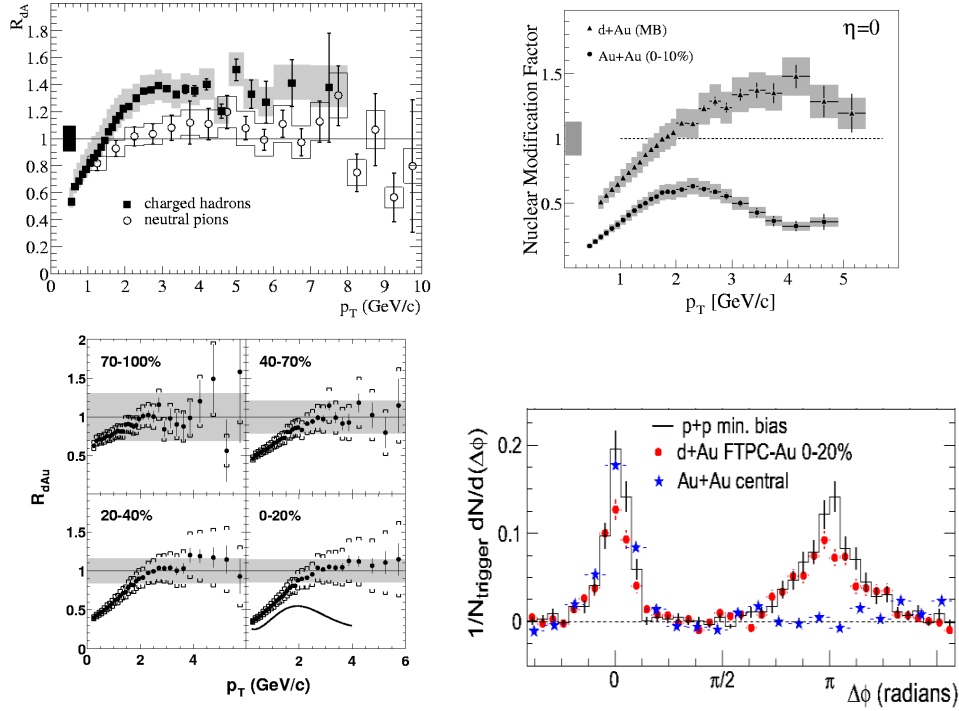


Fig. 16: Top: Nuclear modification factor  $R_{dAu}$  for MB d+Au:  $h^\pm$  and  $\pi^0$  (PHENIX, *left*),  $h^\pm$  (BRAHMS, *right*). Bottom:  $R_{dAu}$  for  $h^\pm$  measured by PHOBOS in 4 different d+Au centralities (*left*), and comparison of two-particle azimuthal distributions for central d+Au, p+p, and central Au+Au collisions (STAR, *right*).

Theoretical predictions of a strong saturation of the nuclear wave function at high energies are also in agreement with most of the data but do not seem to explain consistently Au+Au and d+Au RHIC results at midrapidity. Coming ion-ion runs at RHIC and, in the mid-term, Pb+Pb collisions at LHC energies will help to further strengthen our current understanding of the physics of QCD media at high energy densities.

## References

- [1] See e.g. F. Karsch, Lect. Notes Phys. **583** (2002) 209; hep-lat/0106019.
- [2] See e.g. E. Iancu and R. Venugopalan, hep-ph/0303204, for a recent review.
- [3] K. Adcox *et al.* [PHENIX Collaboration], Phys. Rev. Lett. **88** (2002) 022301.
- [4] C. Adler *et al.*, Phys. Rev. Lett. **89** (2002) 202301, nucl-ex/0206011.
- [5] K. Adcox *et al.* [PHENIX Collaboration], Phys. Lett. **B561** (2003) 82, nucl-ex/0207009.
- [6] S.S. Adler *et al.* [PHENIX Collaboration], Phys. Rev. Lett. **91** (2003) 072301; nucl-ex/0304022.
- [7] J. Adams *et al.* [STAR Collaboration], submitted to Phys. Rev. Lett. , nucl-ex/0305015.
- [8] S. S. Adler *et al.* [PHENIX Collaboration], submitted to Phys. Rev. Lett. , nucl-ex/0308006.
- [9] B. B. Back *et al.* [PHOBOS Collaboration], submitted to Phys. Lett. **B**, nucl-ex/0302015.
- [10] I. Arsene *et al.* [BRAHMS Collaboration], Phys. Rev. Lett. **91** (2003) 072305, nucl-ex/0307003.
- [11] K. Adcox *et al.* [PHENIX Collaboration], Phys. Rev. Lett. **88** (2002) 242301.

- [12] S.S. Adler *et al.* [PHENIX Collaboration], to appear in Phys. Rev. Lett. , nucl-ex/0305036.
- [13] J. Adams *et al.* [STAR Collaboration], submitted to Phys. Rev. Lett. , nucl-ex/0306007.
- [14] B. Alper *et al.*, Nucl. Phys. **B100** (1975) 237.
- [15] A.L.S. Angelis *et al.*, Phys. Lett. **B185** (1987) 213.
- [16] P. Abreu *et al.* [DELPHI Collaboration], Eur. Phys. J. **C17** (2000) 207.
- [17] C. Adler *et al.* [STAR Collaboration], Phys. Rev. Lett. **90** (2003) 082302, nucl-ex/0210033.
- [18] M. Chiu [PHENIX Collaboration], Nucl. Phys. **A715** (2003) 761, nucl-ex/0211008.
- [19] C. Adler *et al.* [STAR Collaboration], Phys. Rev. Lett. **90** (2003) 032301, nucl-ex/0206006.
- [20] S. S. Adler *et al.* [PHENIX Collaboration], to appear in Phys. Rev. Lett. , nucl-ex/0305013.
- [21] S. S. Adler *et al.* [PHENIX Collaboration], Phys. Rev. Lett. **91**, (2003) 072303, nucl-ex/0306021.
- [22] J. Adams *et al.* [STAR Collaboration], Phys. Rev. Lett. **91** (2003) 072304, nucl-ex/0306024.
- [23] B. B. Back *et al.* [PHOBOS Collaboration], Phys. Rev. Lett. **91** (2003) 072302, nucl-ex/0306025.
- [24] D. Antreasyan *et al.*, Phys. Rev. **D19** (1979) 764.
- [25] M. Gyulassy and M. Plümer, Phys. Lett. **B243** (1990) 432; X.N. Wang and M. Gyulassy, Phys. Rev. Lett. **68** (1992) 1480; R. Baier *et al.*, Phys. Lett. **B345** (1995) 277.
- [26] D. Kharzeev, E. Levin and L. McLerran, Phys. Lett. **B561**, 93 (2003).
- [27] K. Gallmeister, C. Greiner and Z. Xu, Phys. Rev. **C67** (2003) 044905.
- [28] R. C. Hwa and C. B. Yang, Phys. Rev. **C 67** (2003) 034902; V. Greco, C. M. Ko and P. Levai, Phys. Rev. Lett. **90** (2003) 202302, R. J. Fries, B. Muller, C. Nonaka and S. A. Bass, Phys. Rev. Lett. **90** (2003) 202303.
- [29] M. Gyulassy, I. Vitev and X. N. Wang Phys. Rev. Lett. **86** (2001) 2537.
- [30] Y. V. Kovchegov and K.L. Tuchin Nucl. Phys. **A708** (2002) 413; Nucl. Phys. **A717** (2003) 249.
- [31] D. Molnar and S. A. Voloshin, Phys. Rev. Lett. **91** (2003) 092301.
- [32] C. Albajar *et al.* [UA1 Collaboration], Nucl. Phys. **B335** (1990) 261.
- [33] S.S. Adler *et al.* [PHENIX Collaboration], hep-ex/0304038.
- [34] G.G. Barnafoldi, P. Levai, G. Papp, G. Fai, and Y. Zhang, nucl-th/0212111.
- [35] J. Rak [PHENIX Collaboration], Proceeds. Int. Conf. on High-Energy Interactions: Theory and Experiment (Hadron Structure '02), Herlany, Slovakia, 22-27 Sep 2002; nucl-ex/0306031.
- [36] A. L. Angelis *et al.* [CERN-Columbia-Oxford-Rockefeller Collab.], Phys. Lett. **B97** (1980) 163.
- [37] L. Apanasevich *et al.*, Phys. Rev. **D59** (1999) 074007, hep-ph/9808467.
- [38] A. Bialas, M. Bleszynski and W. Czyz, Nucl. Phys. **B111** (1976) 461.
- [39] K. Adcox *et al.* [PHENIX Collaboration], Phys. Rev. Lett. **86** (2001) 3500.

- [40] B. B. Back *et al.* [PHOBOS Collaboration], Phys. Rev. **C65** (2002) 061901, nucl-ex/0201005.
- [41] S. Jeon, J. Jalilian-Marian and I. Sarcevic, Phys. Lett. **B562** (2003) 45.
- [42] D. d'Enterria [PHENIX Collaboration], Nucl. Phys. **A715** (2003) 749.
- [43] I. Vitev and M. Gyulassy, Phys. Rev. Lett. **89** (2002) 252301.
- [44] X. N. Wang, nucl-th/0305010.
- [45] F. Arleo, J. High Energy Phys. **11** (2002) 44.
- [46] C. A. Salgado and U. A. Wiedemann, Phys. Rev. **D68** (2003) 014008; hep-ph/0302184.
- [47] M.M. Aggarwal *et al.* [WA98 collab.], Eur. Phys. J. **C23** (2002) 225.
- [48] K. J. Eskola, V. J. Kolhinen and C. A. Salgado, Eur. Phys. J. **C 9** (1999) 61.
- [49] S. R. Klein and R. Vogt, Phys. Rev. **C67** (2003) 047901.
- [50] R. Baier, D. Schiff, B.G. Zakharov, Ann. Rev. Nucl. Part. Sci. **50** (2000) 37.
- [51] M. Gyulassy, P. Levai and I. Vitev, Phys. Rev. Lett. **85** (2000) 5535, Nucl. Phys. **B594** (2001) 371.
- [52] D. d'Enterria [PHENIX Collaboration], Proceeds. 19th Winter Workshop on Nuclear Dynamics, Breckenridge (CO), 9-15 Feb 2003; nucl-ex/0306001.
- [53] X. N. Wang, nucl-th/0307036.
- [54] B. Muller, arXiv:nucl-th/0208038.
- [55] P. Jacobs and J. Klay, nucl-ex/0308023.
- [56] E. V. Shuryak, Phys. Rev. **C 66** (2002) 027902, nucl-th/0112042.